Figure 1

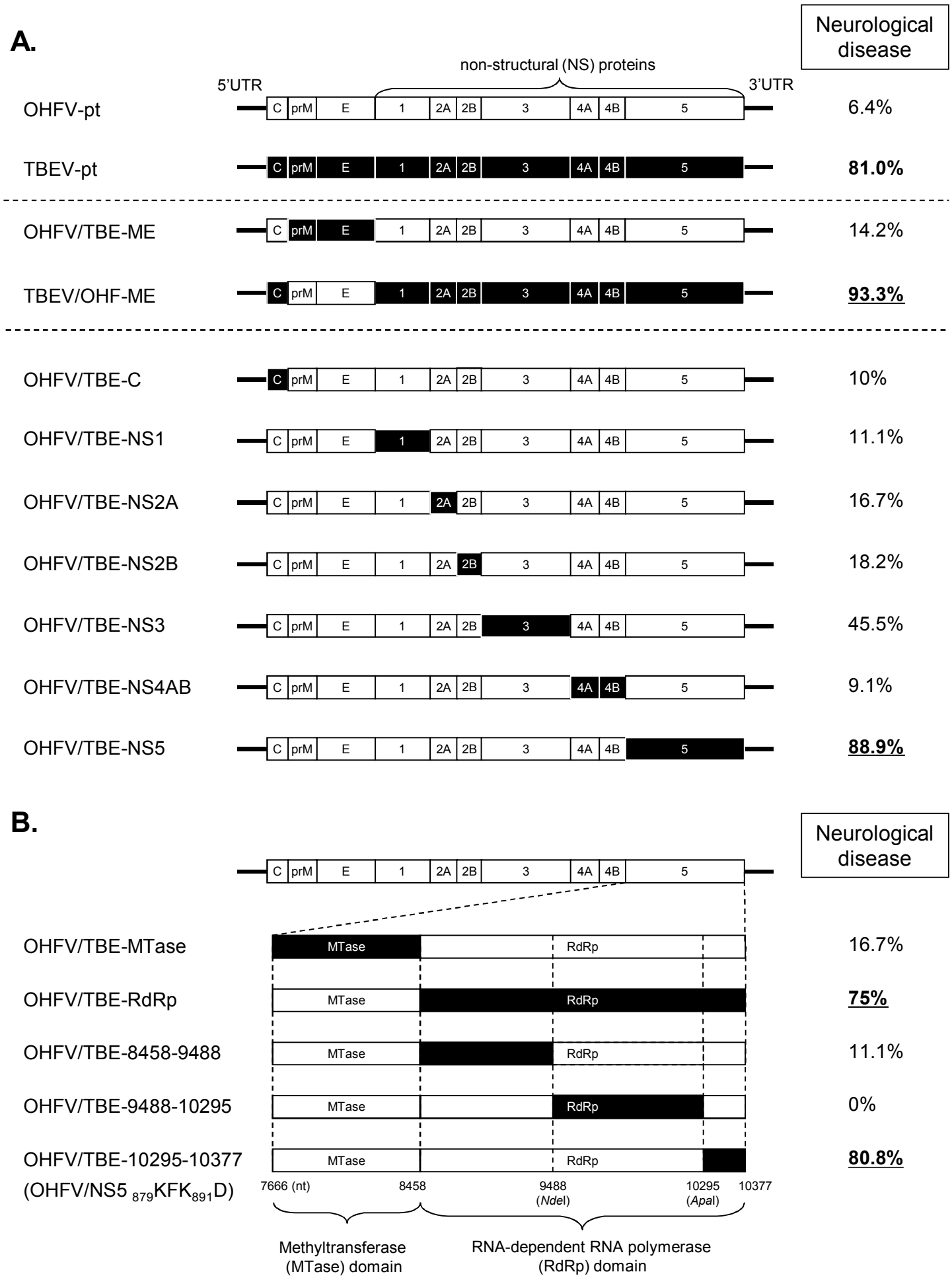
A.
Neurological disease
non-structural (NS) proteins
5'UTR
3'UTR
C prM E 1 2A 2B 3 4A 4B 5
OHFV-pt
6.4%
TBEV-pt
81.0%
OHFV/TBE-ME
14.2%
TBEV/OHF-ME
93.3%
OHFV/TBE-C
10%
OHFV/TBE-NS1
11.1%
OHFV/TBE-NS2A
16.7%
OHFV/TBE-NS2B
18.2%
OHFV/TBE-NS3
45.5%
OHFV/TBE-NS4AB
9.1%
OHFV/TBE-NS5
88.9%
B.
Neurological disease
MTase
RdRp
OHFV/TBE-MTase
16.7%
OHFV/TBE-RdRp
75%
OHFV/TBE-8458-9488
11.1%
OHFV/TBE-9488-10295
0%
OHFV/TBE-10295-10377
80.8%
(OHFV/NS5 879KFK891D)
7666 (nt)
8458
9488 (NdeI)
10295 (ApaI)
10377
Methyltransferase (MTase) domain
RNA-dependent RNA polymerase (RdRp) domain

Figure 1

C.

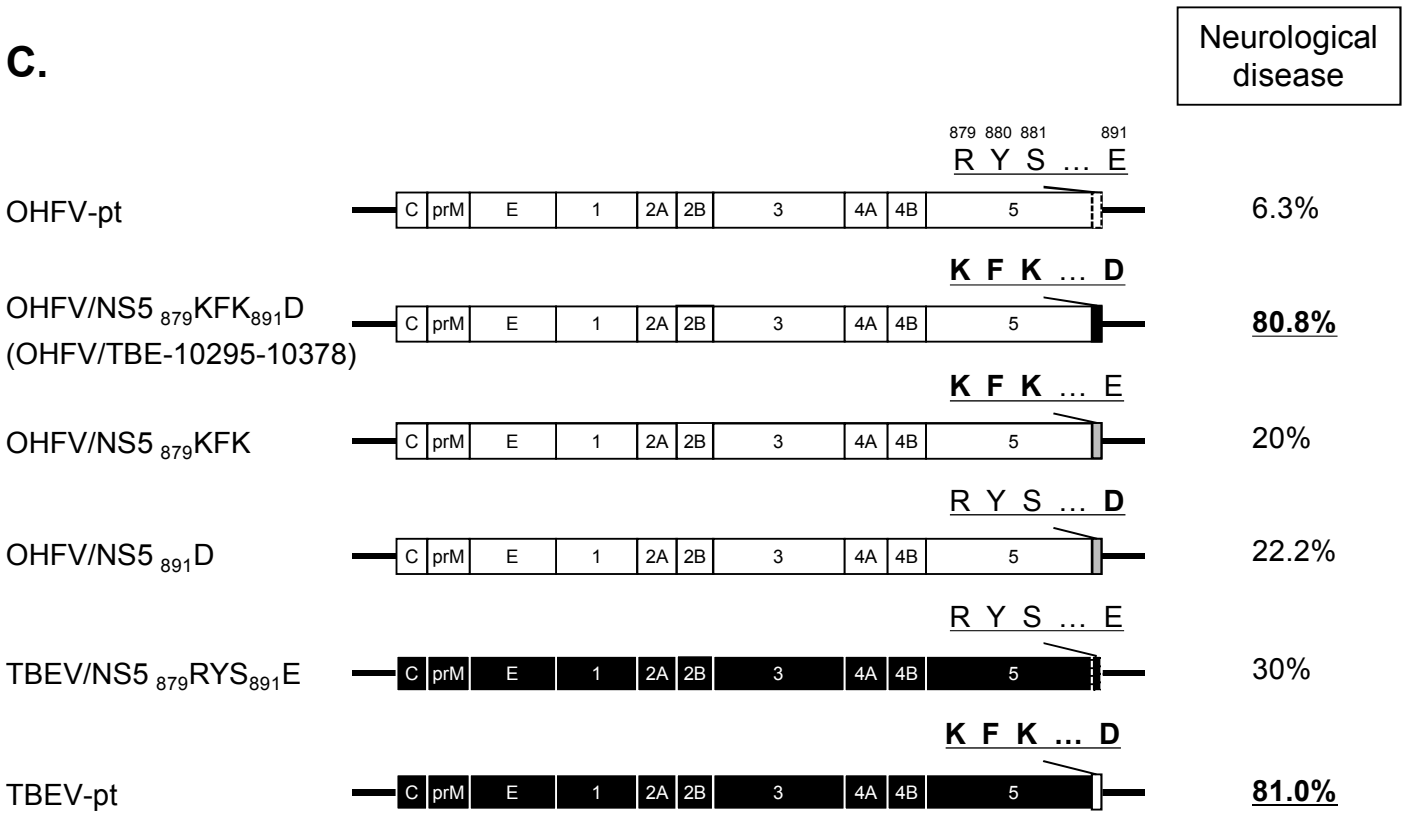

Figure 1.

Neurological disease in mice infected with chimeric viruses.

The coding regions for OHFV and TBEV proteins are shown in white and black, respectively. The percentages of mice exhibiting signs of neurological disease are shown on the right. (A) Chimeric viruses were constructed by replacement of the coding region for each viral protein. (B) The coding region of OHFV non-structural protein NS5 was partially replaced with that of TBEV; nucleotide positions and restriction enzyme sites used for this replacement are indicated. (C) The amino acids at positions 879, 880, 881, and/or 891 of NS5 were substituted. Normal and bold letters indicate the amino acid sequences of OHFV and TBEV, respectively.

Figure 2

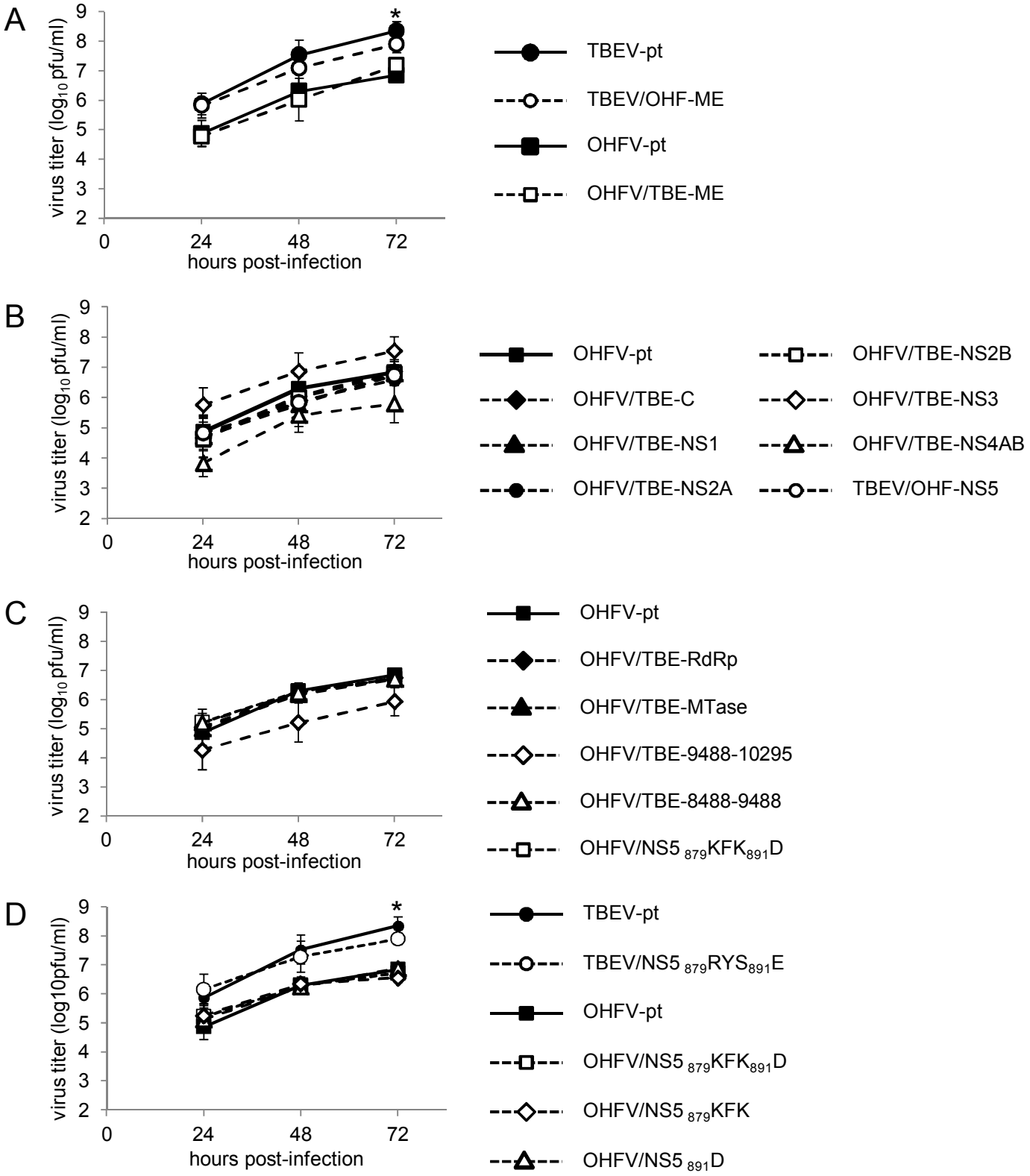

Figure 2. **Growth curves of chimeric viruses.**
A Monolayer of BHK-21 cells was infected with wild-type and chimeric viruses at a multiplicity of infection (MOI) of 0.01. Media were harvested at each time point, and viral titers determined by plaque assay in BHK-21 cells. The chimeric viruses showed no significant differences from parental virus at any time point examined.
(A) Chimeric viruses with replacement of viral envelope proteins (prM/E). * indicates significant difference between TBEV-pt and OHFV-pt, and between TBEV-pt and OHFV/TBE-ME ($P < 0.05$).
(B) Chimeric OHFV with replacement of the C or each NS protein.
(C) Chimeric OHFV with partial replacement in the NS5 protein.
(D) Chimeric viruses with substitutions in the KFK-D motif. * indicates a significant difference between TBEV-pt and all chimeric OHFV ($P < 0.05$).

Figure 3

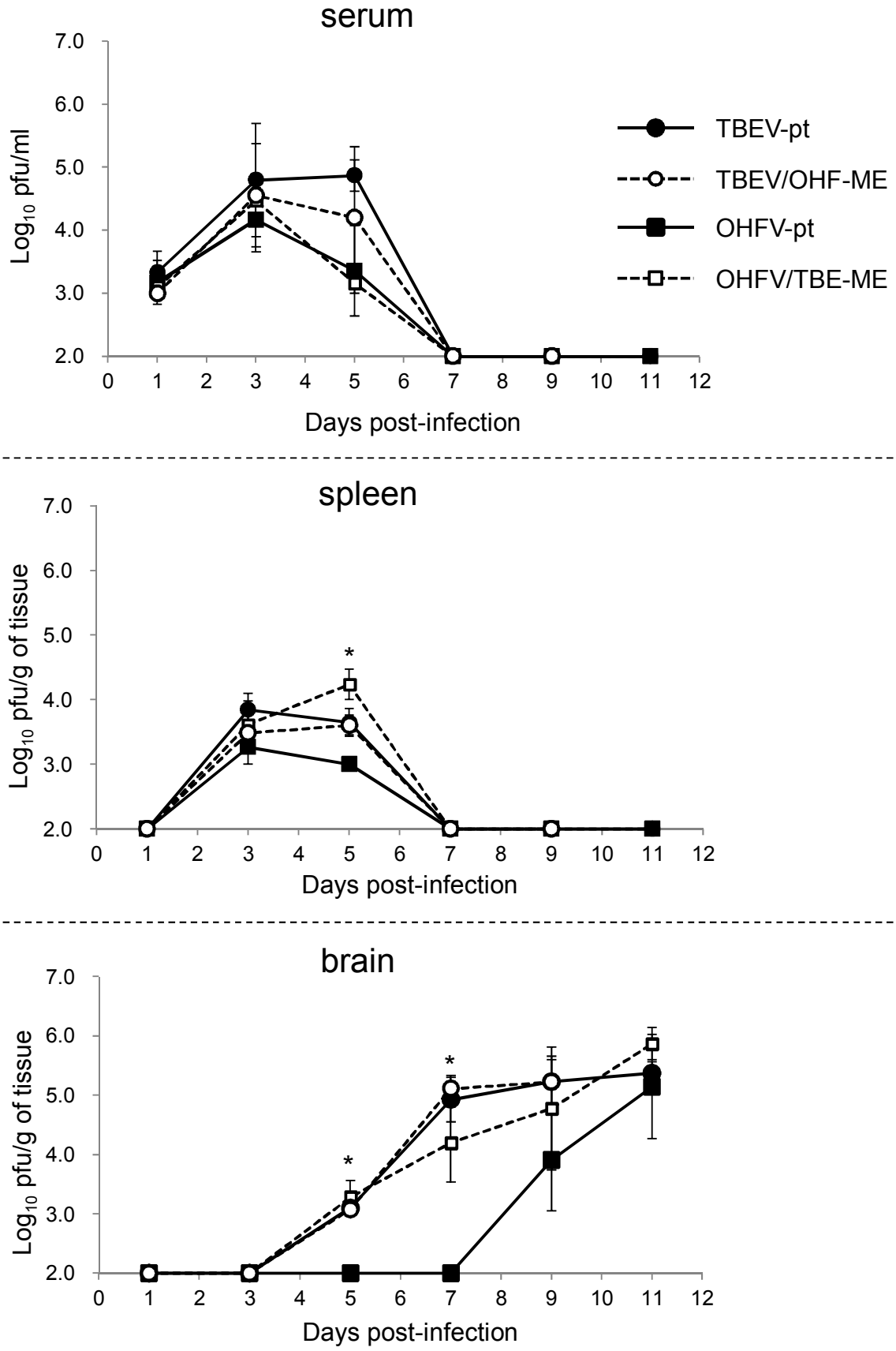

Figure 3.

Multiplication in organs of chimeric viruses following replacement of the envelope proteins. Mice were infected with 10,000 pfu of each virus (TBEV-pt, TBEV/OHF-ME, OHFV-pt, and OHFV/TBE-ME). Viral titers in serum, spleen, and brain were determined by plaque assays on the days indicated. Error bars represent the SD ($n = 4$). By 11 dpi, all mice inoculated with TBEV/OHF-ME had died. * indicates a significant difference between TBEV-pt and OHFV-pt ($P < 0.05$). No significant differences were observed between TBEV-pt, TBEV/OHF-ME and OHF/TBE/ME.

Figure 4

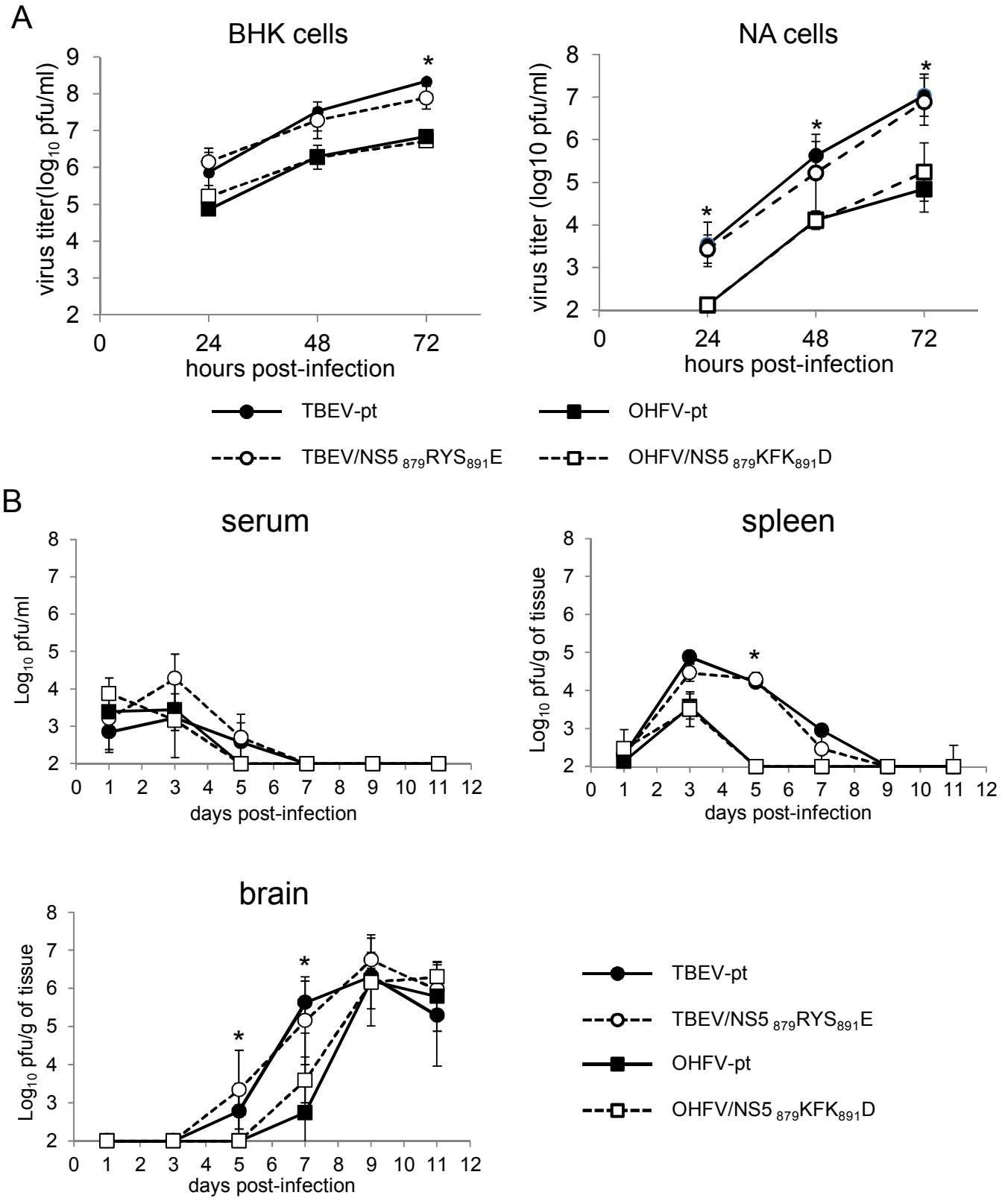

Figure 4.

Growth properties of chimeric viruses containing NS5 amino acid substitutions.

A. Monolayers of BHK-21 or NA cells were infected with wild-type and chimeric viruses at a multiplicity of infection (MOI) of 0.01. Media were harvested at each time point, and viral titers were determined by plaque assay in BHK-21 cells.

B. Mice were infected with 10,000 pfu of each virus. Viral titers in serum, spleen, and brain were determined by plaque assays on the days indicated. Error bars represent the SD ($n = 3$). * indicates significant difference between TBEV-pt and OHFV-pt, and between TBEV-pt and OHFV/NS5 $_{879}$KFK$_{891}$D ($P < 0.05$). No significant differences were observed between TBEV-pt and TBEV/NS5 $_{879}$RYS$_{891}$E, or between OHFV-pt and OHFV/NS5 $_{879}$KFK$_{891}$D at any time-points.

Figure 5

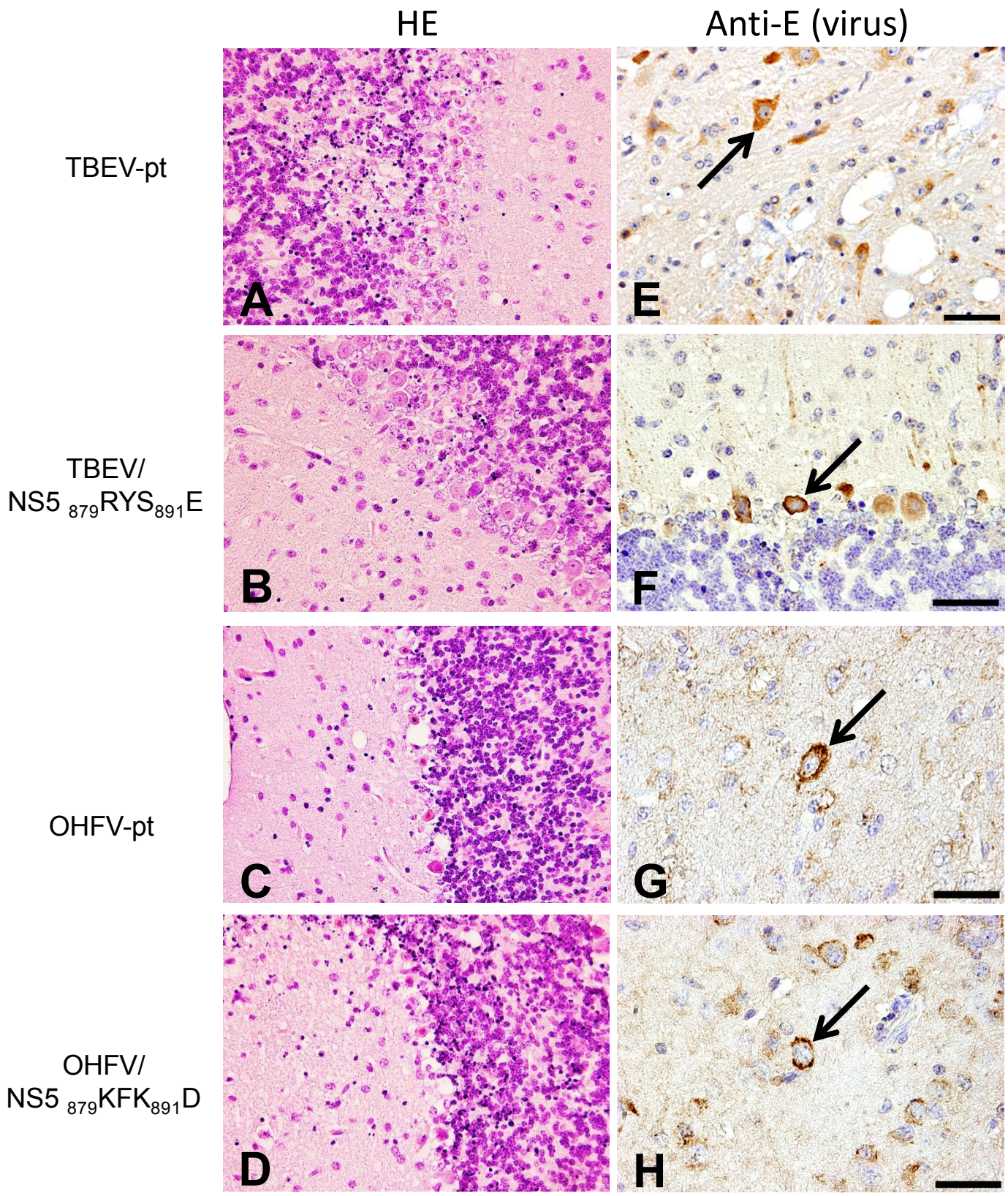

Figure 5.
Mice were inoculated with 10,000 pfu of TBEV-pt (A and E), TBEV/NS5 $_{879}$RYS$_{891}$E (B and F), OHFV-pt (C and G), or OHFV/NS5 $_{879}$KFK$_{891}$D (D and H), and sacrificed at terminal stages of disease (7 - 13 dpi). Brain histopathology consisted of marked non-suppurative encephalitis in all mice. Severe tissue damage with degeneration and necrosis of Purkinje cells, and pyknosis of granule cells in the cerebellum (A - D, original magnification ×400). Viral antigens (arrows) were detected in the cytoplasm of various neuronal cells in the brains of virus-infected mice (E - H, bars = 50 μm).

Figure 6

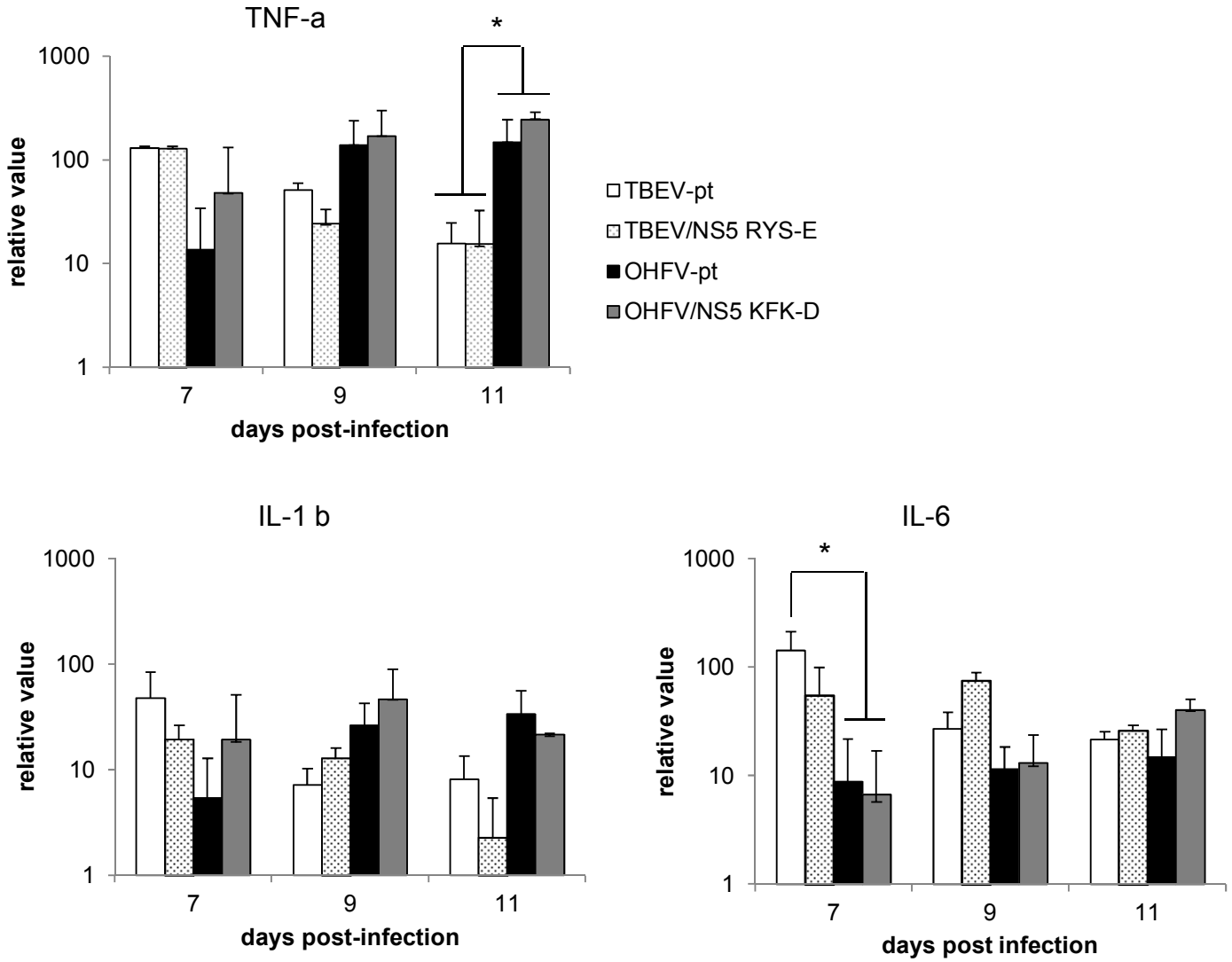

Figure 6.

Expression of inflammatory cytokines in the brains of mice infected with chimeric viruses.

Mice were inoculated with 10,000 pfu of TBEV-pt, TBEV/NS5 $_{879}$RYS$_{891}$E, OHFV-pt, or OHFV/NS5 $_{879}$KFK$_{891}$D, and the expression of inflammatory cytokines in the brain was measured by real-time PCR. The levels of TNF-α, IL-1β, and IL-6 mRNA expression were measured at the time points indicated, and normalized against GAPDH. Expression levels are shown relative to uninfected controls. * indicates a significant difference ($P < 0.05$).

Figure 7

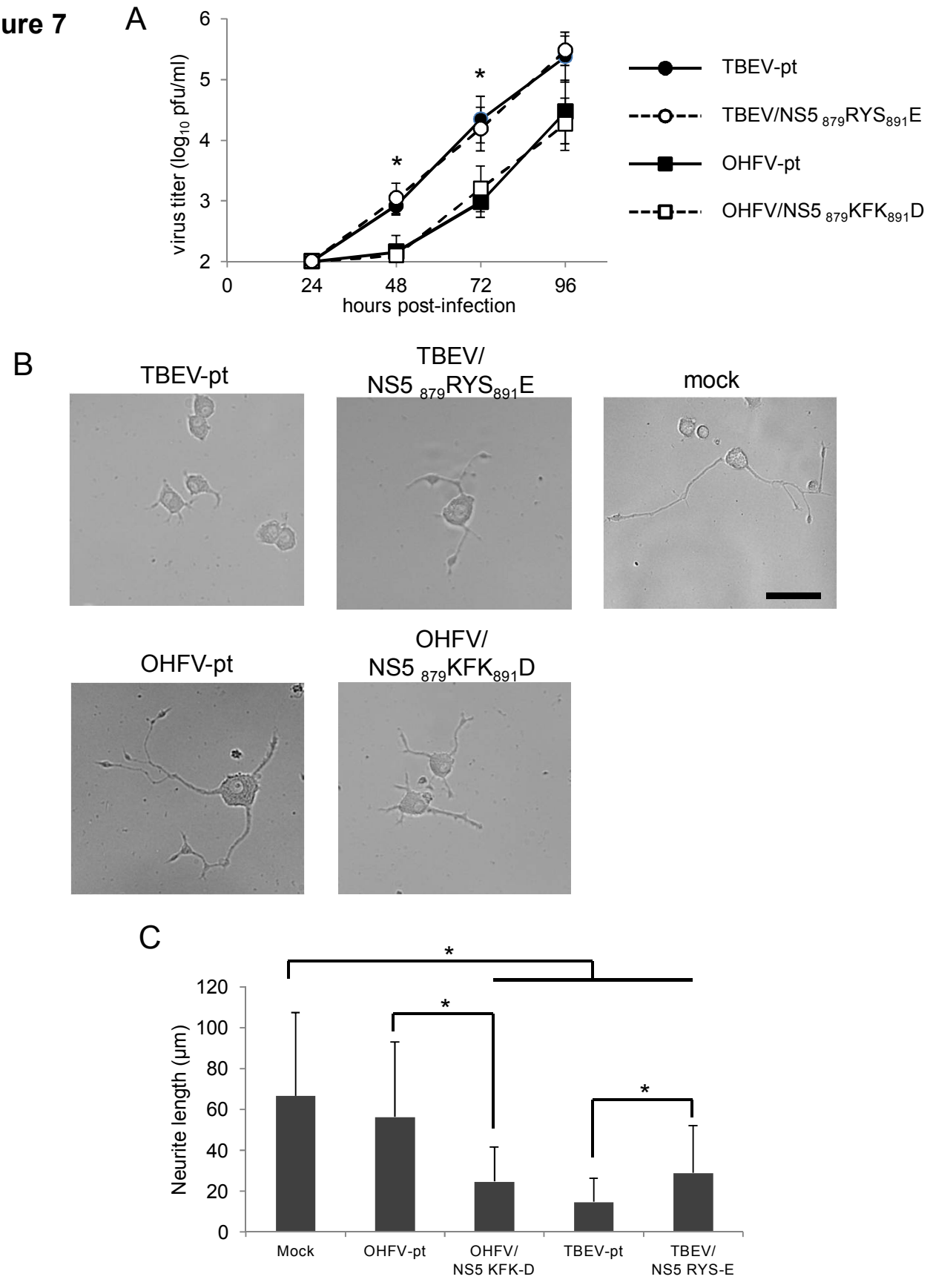

Figure 7.

Neurite formation by PC12 cells infected with chimeric viruses containing NS5 amino acid substitutions. PC12 cells were infected with TBEV-pt, TBEV/NS5 $_{879}$RYS$_{891}$E, OHFV-pt, or OHFV/NS5 $_{879}$KFK$_{891}$D at a multiplicity of infection (MOI) of 10, and were treated with 150 ng/mL NGF at 24 hours post-infection.

A. Media were harvested at each time point, and viral titers were determined by plaque assay in BHK-21 cells. * indicates a significant difference between TBEV-pt and OHFV-pt, and between TBEV-pt and OHFV/NS5 $_{879}$KFK$_{891}$D ($P < 0.05$). No significant differences were observed between TBEV-pt and TBEV/NS5 $_{879}$RYS$_{891}$E, or between OHFV-pt and OHFV/NS5 $_{879}$KFK$_{891}$D at any time point.

Figure 8

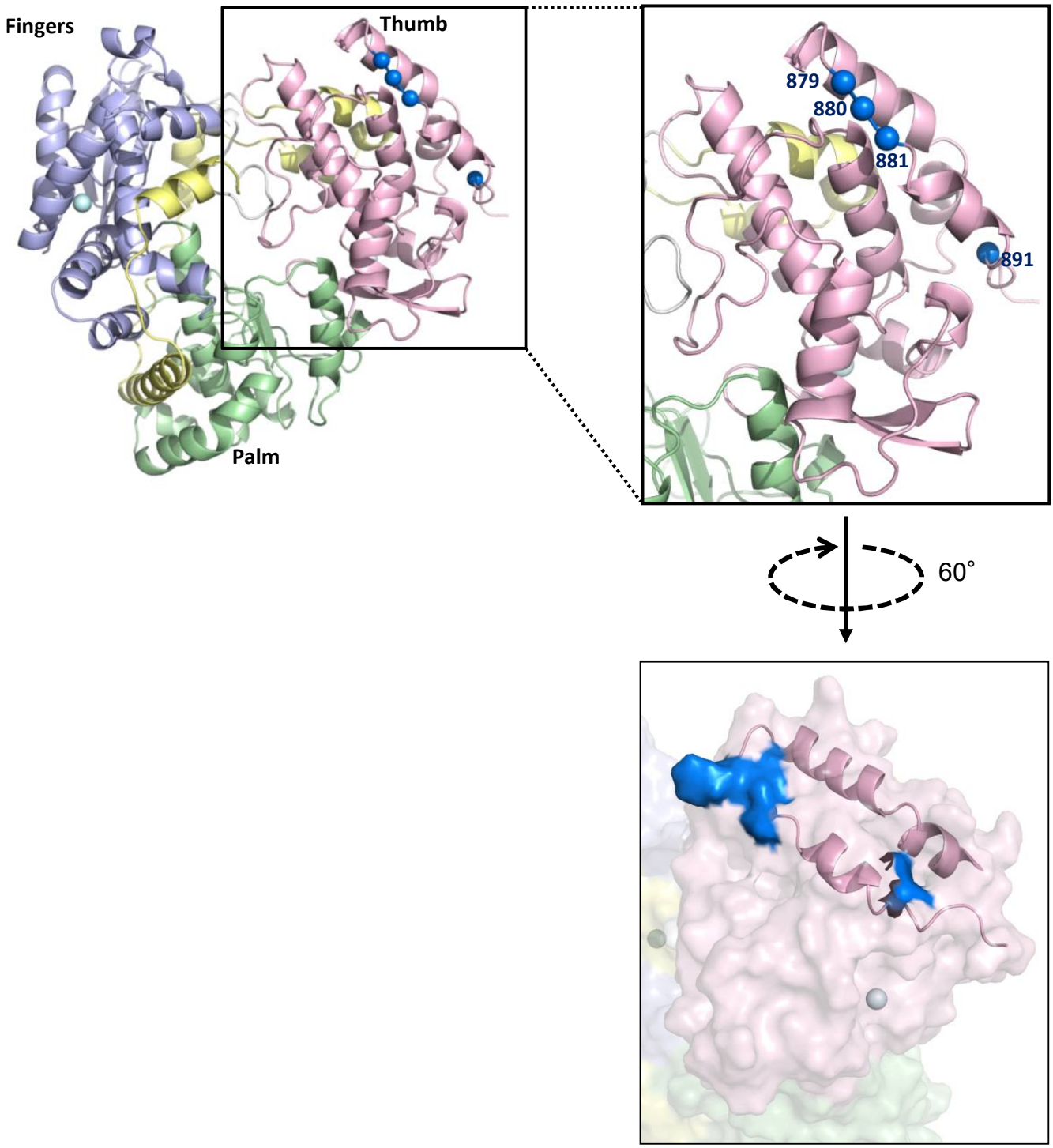

Figure 8.
Amino acids involved in the neurological disease caused by tick-borne flaviviruses.
A three-dimensional model of the tick-borne flavivirus RNA-dependent RNA polymerase domain in NS5 was constructed based on the crystal structure of West Nile virus polymerase (PDB code: 2HFZ). The structure of tick-borne flavivirus polymerase is shown in ribbon (upper) and surface (lower) representations. Amino acid positions 879, 880, 881, and 891 are colored blue.